Acoustic gain in piezoelectric semiconductors at -near-zero response

Willatzen, Morten; Christensen, Johan

Published in:
Physical Review B (Condensed Matter and Materials Physics)

Link to article, DOI:
10.1103/PhysRevB.89.041201

Publication date:
2014

Document Version
Publisher's PDF, also known as Version of record

PHYSICAL REVIEW B **89**, 041201(R) (2014)

Acoustic gain in piezoelectric semiconductors at ε-near-zero response

M. Willatzen[1,*] and J. Christensen[1,2]

[1]*Department of Photonics Engineering, Technical University of Denmark, DK-2800 Kgs. Lyngby, Denmark*

[2]*Institute of Technology and Innovation, University of Southern Denmark, DK-5230 Odense, Denmark*

(Received 13 November 2013; revised manuscript received 10 January 2014; published 27 January 2014)

We demonstrate strong acoustic gain in electric-field biased piezoelectric semiconductors at frequencies near the plasmon frequency in the terahertz range. When the electron drift velocity produced by an external electric field is higher than the speed of sound, Cherenkov radiation of phonons generates amplification of sound. It is demonstrated that this effect is particularly effective at ε-near-zero response, leading to giant levels of acoustic gain. Operating at conditions with strong acoustic amplification, we predict unprecedented enhancement of the scattered sound field radiated from an electrically controlled piezoelectric slab waveguide. This extreme sound field enhancement in an active piezo material shows potential for acoustic sensing and loss compensation in metamaterials and nonlinear devices.

DOI: 10.1103/PhysRevB.89.041201 PACS number(s): 77.84.−s, 73.20.Mf, 81.05.Xj, 85.50.−n

Active materials producing electromechanical coupling can be achieved by piezoelectric (PZ) structures but can also be realized by means of electrostriction and thermoelectromechanical effects. If a PZ material undergoes mechanical deformations, it produces electric charges, and vice versa, when an electric field is applied, the structure is mechanically strained. Commonly, PZ materials are found to be made of both natural and synthesized crystals, among which we can name ferroelectric oxides, quartz, Rochelle salt, and synthetic ceramics such as lead titanate, zinc oxide, and bismuth ferrite. Today there exist numerous versatile applications based on PZ sensors, actuators, and switches used for the automotive industry, medical instruments, and telecommunications. On a more fundamental aspect, PZ semiconductors play a crucial role, and it is believed that this discipline offers a plethora of yet unseen electromechanical effects within a high-frequency regime. Nanopiezotronics and nanopyroelectrics, for example, comprise the study of thermal and electromechanical properties associated with wurtzite-compound or ferroelectric nanowires and nanobelts with high functionalities for the use in diodes, transistors, and nanogenerator systems, among many other applications [1–9]. Mechanical strain and displacements are important tuning paradigms in many of these named functions. For this reason, it is important to acquire basic insights into electromechanical coupling since it governs the electronic, mechanical, and optical properties of many nano- and microsized PZ structures. One among many intriguing coupling schemes is the one capable of producing acoustic gain.

Amplification of mechanical waves (sound) was observed by Hutson *et al.* in 1961 in a CdS semiconductor slab [10]. When an acoustic field, upon external irradiation, deforms the PZ material, space charges are generated by the elastic field and cause the electrons to redistribute accordingly. The electron drift induced by an external field can become supersonic, that is, $v_d > v_s$ [where $v_s(v_d)$ is the sound (electron drift) velocity], and amplification can take place due to the phonon emission of carriers [11–13]. In other words, acoustic gain is produced when the electron drift velocity exceeds the velocity of sound, which is in direct analogy to Cherenkov radiation. From the constitutive PZ relations, it can be shown that the electromechanical stress $\mathcal{T}$ is inversely proportional to the dielectric constant ε in the absence of a net charge in the semiconductor. The presence of acoustically generated charge carriers will, however, modify this result slightly. It then follows that elastic strains such as acoustic amplification can be boosted significantly when tuned toward ε-near-zero (ENZ) response.

In this Rapid Communication we present a seminumerical study of the amplification process of sound in PZ semiconductor materials. We distinguish between a low-frequency regime where acoustic gain unambiguously is explained by the emission of sound due to Cherenkov radiation and a high-frequency one where ε approaches zero. In ENZ materials, light propagates with almost no phase advance due to the extended sizes of the wavelength [14,15]. This has been achieved by metamaterials and has resulted in prominent applications such as supercoupling and directive emission of light and sensing, to name a few [16]. In the context of PZ acoustic amplification at ENZ response, we show that gain can be many orders of magnitude larger compared to amplification caused by Cherenkov emission. In addition, we design an optomechanical device giving rise to enhanced acoustic radiation triggered by electrical switching with the cycle of half a wave round-trip.

Consider the constitutive relations for a piezoelectric material,

$$\begin{aligned} \mathcal{T} &= cS - eE, \\ D &= \varepsilon E + P + eS, \end{aligned} \tag{1}$$

where $\mathcal{T}$, S, D, E, P, c, e, and ε are the stress, strain, electric displacement, electric field, spontaneous polarization, stiffness, piezoelectric e constant, and permittivity, respectively. In cubic (zinc blende) structures the spontaneous polarization is zero, but in hexagonal (wurtzite) structures the spontaneous polarization is nonzero and is usually higher than the piezoelectric contribution to the electric displacement. In reality, the above equations are tensor equations for the crystal;

*morwi@fotonik.dtu.dk

however, discarding field variations in space except along one coordinate, z, the above scalar system suffices for the analysis.

The constitutive relations above are for isentropic conditions such that Onsager relations apply. This approximation will only be used in the constitutive relations, and losses are accounted for by using a finite and frequency-dependent complex carrier mobility. The elastic equation in one dimension is

$$\rho\frac{\partial^2 u}{\partial t^2}=\frac{\partial \mathcal{T}}{\partial z}=c\frac{\partial^2 u}{\partial z^2}-e\frac{\partial E}{\partial z}, \tag{2}$$

where ρ and ω are the mass density and angular frequency, respectively, and $S=\frac{\partial u}{\partial z}$, with u being the material displacement. We consider only electrons as the acoustic response of the much heavier holes can be discarded. The continuity equation reads

$$\frac{\partial J}{\partial z}=-\frac{\partial \rho_e}{\partial t},\qquad J=q\mu_n nE+qFD_n\frac{\partial n_s}{\partial z}, \tag{3}$$

where J and ρ_e are the free-current density and the space-charge density, respectively, F denotes the fraction of acoustically generated electrons that are free to move, q is the elementary charge, μ_n is the electron mobility, D_n is the electron diffusivity, and $n=n_0+n_s$, n_s, and n_0 are the total electron density, the generated acoustic electron density, and the electron density at equilibrium, respectively. Combining the above expressions implies an electromechanical dispersion relation:

$$\rho\omega^2=ck^2-\frac{k^2e^2}{\frac{iqn_0\mu_n}{\omega+F\mu_nE_0k-iFD_nk^2}-\varepsilon}. \tag{4}$$

This equation is a fourth-order complex polynomial in $k=\frac{\omega}{v_s}-i\alpha$, where α is the damping term. Now, since $|\alpha|\ll\frac{\omega}{v_s}$, we may safely, for small fields E_0, replace k by $\frac{\omega}{v_s}$ in the denominator of the second term on the right-hand side. The resulting dispersion equation is a second-order polynomial in k whose roots we denote k_1 and k_2 henceforth. The dispersion relation is supplemented by a Drude permittivity frequency response for semiconductors,

$$\varepsilon=\varepsilon_\infty\left(1-\frac{\omega_p^2}{\omega^2+\tau^{-2}}\right), \tag{5}$$

where ω_p is the plasmon frequency and the complex mobility μ_n is

$$\mu_n=\mu_{DC}\frac{\tau^{-1}}{\tau^{-1}+i\omega}, \tag{6}$$

where μ_{DC} is the dc mobility and τ is the carrier collision time. We note that either the plasmon frequency or the collision time (or both) are in the terahertz (THz) range for many semiconductors so that the permittivity approaches zero and changes sign only in the range of THz frequencies. A strong mechanical response within this spectral range is predicted since vanishing permittivities lead to a tremendously high stress, $T\sim 1/\varepsilon$, as derived from Eq. (1), and is responsible for obtaining enhanced gain or absorption, which we will see in the following. The above dispersion relation is solved for the case of zinc-blende InSb using the following parameters: $e=-0.07$ C/m^2, $c=4.7\times10^{10}$ Pa, $m_{\text{eff}}=0.014$ (in units of the free-electron mass), $\rho=5770$ kg/m^3, $n_0=2\times10^{22}$ m^{-3}, $\mu_{DC}=7.7$ m^2 s^{-1} V^{-1}, $\varepsilon_\infty=15.7$, $\tau=m_{\text{eff}}\mu_{DC}/q$, and $F=1$, corresponding to a plasmon frequency $f=2.71$ THz. It is evident from the k_1 wave-number plots in Figs. 1(a) and 1(b) for a frequency range far below the plasmon frequency ω_p that an abrupt transition from absorption to gain occurs near the position where the Cherenkov condition is fulfilled, i.e., where the drift speed $v_d=\mu E_0$ surpasses the speed of sound v_s. The small deviation in the transition frequency away from the Cherenkov condition stems from the appearance of the small diffusion term in Eq. (4). Gain (absorption) requires the real and imaginary terms of the wave vector to have the same (opposite) sign [refer to Fig. 1(b)]. In the case of InSb and the parameters above, the transition between absorption and gain takes place when the dc electric field equals approximately -430 V/m. It is also evident from Fig. 1(a) that the strength of the gain or absorption is weak since the damping term of k_1 is at most 0.005 m^{-1}, with increasing gain toward increasing electric field strength and low frequencies. In Figs. 1(c) and 1(d), we also plot the wave-number component k_2. Since the real and imaginary components are always of opposite sign irrespective of the dc electric field value, only absorption is possible for this mode, and k_2 excitations are always damped during propagation. Further, it can be seen that the absorption strength is rather weak for k_2 modes, a result that is similar to earlier absorption results [11].

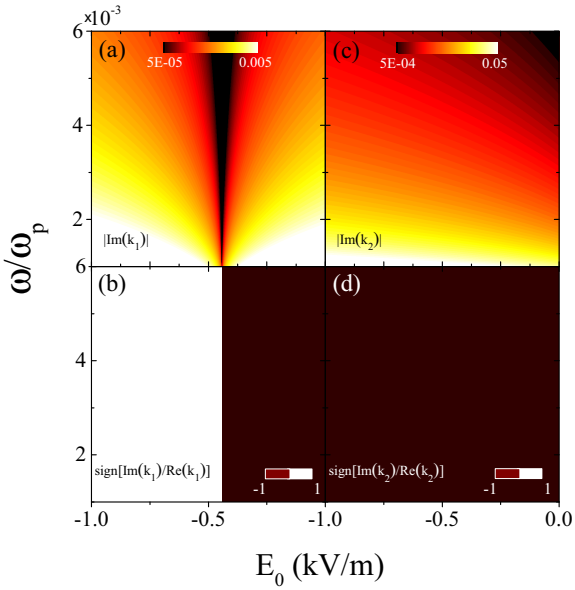

FIG. 1. (Color online) Weak response at low frequencies for InSb, far below the plasmon frequency $f=2.71$ THz. The wave numbers k_1 and k_2 are calculated as a function of electric field and normalized frequency ω/ω_p. (a) $|\text{Im}(k_1)|$ and (b) illustrating the sign of the ratio of the real and imaginary parts of k_1. (c) and (d) The same as (a) and (b), but for k_2. Color bar units are in m^{-1}.

Similar plots of k_1 and k_2 are shown in Fig. 2 for frequencies around the plasmon frequency. It follows from Eq. (4) that when $\varepsilon=0$ (for a Drude permittivity response this occurs when $\omega^2=\omega_p^2-\tau^2$, assuming $\omega_p>\tau$, as is the case for, e.g., intrinsic InSb), the imaginary part of k can take on arbitrarily

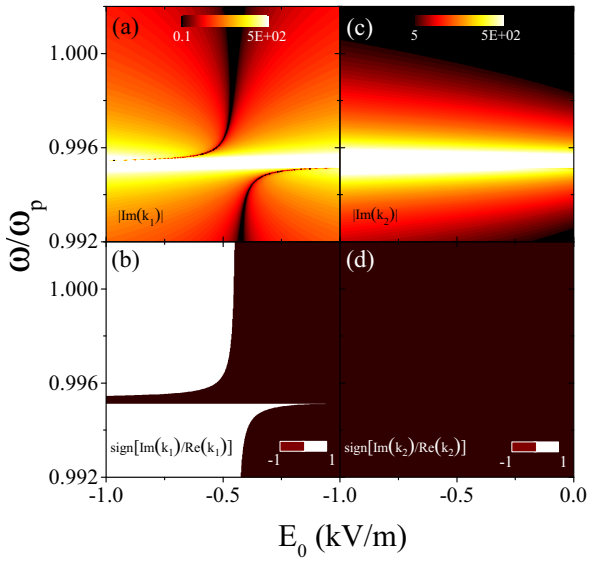

FIG. 2. (Color online) Strong gain at ENZ conditions with frequencies around the plasmon frequency $f = 2.71$ THz for InSb. (a)–(d) The two wave numbers, k_1 and k_2, are captured as in Fig. 1 to demonstrate gain and absorption. Color bar units are in m^{-1}.

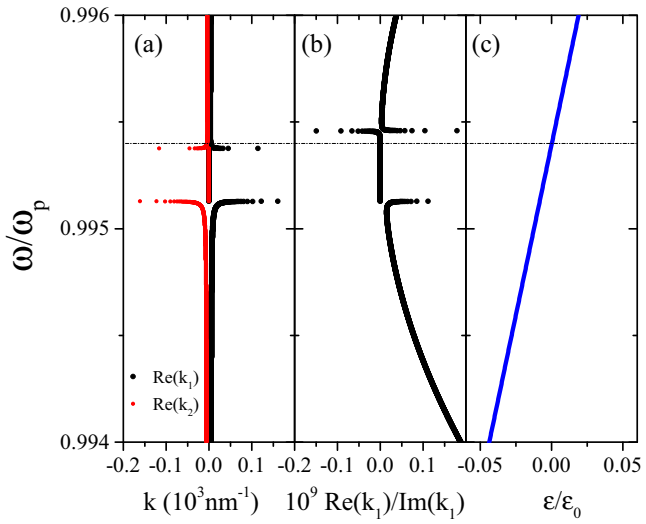

FIG. 3. (Color online) Dispersion relation and spectral dependence of the permittivity for InSb with $E_0 = -1000$ V/m. (a) The real parts of the wave numbers k_1 and k_2 are shown to be symmetric on a dispersion diagram. (b) Gain is present for k_1, as illustrated by $\mathrm{Re}(k1)/\mathrm{Im}(k1)$. (c) $\varepsilon/\varepsilon_0$ plotted near the plasmon frequency $f = 2.71$ THz. The dash-dotted line marks the spectral region where $\varepsilon = 0$.

large positive (or negative) values as the electric field is increased. Thus, we can tailor the intrinsic acoustic absorption or gain by controlling the frequency and the dc electric field. Significant changes appear in the magnitude of the imaginary components of k_1 and k_2. We find a maximum damping $|\mathrm{Im}(k_1)|$ around 500 m^{-1}, i.e., five orders of magnitude higher than that at low frequencies shown previously. Also, compared to the former case, the change from absorption to gain is more complex and not in agreement with the standard Cherenkov condition due to electron diffusion effects. Only the k_1 wave number displays evidence of sound amplification since the condition $\mathrm{Im}(k_1)/\mathrm{Re}(k_1) > 0$ sustains for a broad spectral range, as rendered in Figs. 2(a) and 2(b).

To shed light on this remarkable finding, we compute a complex dispersion relation for InSb with the aforementioned parameters and $E_0 = -1000$ V/m and draw an immediate connection to the spectral dependence of the permittivity around the plasmon frequency, as seen in Fig. 3. The real parts of the wave numbers are shown to be equal in magnitude but of opposite signs, as seen in Fig. 3(a). Due to the frequency dependence of the permittivity and the mobility as well as a finite Drude carrier collision time, k_1 and k_2 reveal strong changes at ENZ but are slightly shifted away from the exact plasmon frequency. This relationship where $\varepsilon = 0$ [Fig. 3(c)] and pronounced dispersion is predicted is accompanied by strong variations in the sign of acoustic damping [Fig. 3(b)] and is illustratively connected by the horizontal dash-dotted line in Fig. 3. It is the strong acoustic gain, whose spectral location remains unaffected by the applied field, as shown in Figs. 2(a) and 2(b), that is directly linked to ENZ response.

We now discuss a principle of an electroacoustic gain device based on a thin slab of semiconductor material controlled by an external dc electric field. It is evident that acoustic gain of a sound field is possible if a substantial part of the sound field enters a thin slab of InSb (or another semiconductor) and if the dc electric field in the slab ensures acoustic gain as the sound traverses the slab in, say, the positive z direction. The basic requirement is to have a high enough applied electric field E_0 and to operate at ENZ conditions so that $|\mathrm{Im}(k_1)|$ is high and damping is positive, $\mathrm{Im}(k_1)/\mathrm{Re}(k_1) > 0$ (refer to Figs. 2 and 3). It is important that the material surrounding the slab of length L is acoustically well matched to guarantee that a high portion of the incoming sound field enters the slab. In Fig. 4(a) we compute the transmission amplitude of an incoming plane wave impinging on a slab when a constant electric field is applied. The surrounding media are assumed to have an acoustic impedance $Z = 3 \times 10^7$ kg/(m^2s), and the plasma frequency is $f = 2.69$ THz. Clearly, due to the exponential increase in the sound field along the positive z direction in a case with gain, the longer the slab is, the higher the transmission coefficient becomes. Calculations at different frequency values again show that amplification is strongest slightly below ω_p. Since the real part of the wave number is considerably larger in magnitude than its imaginary part whenever gain is present, many oscillations in the acoustic field will take place over a slab length where gain is pronounced. This is a drawback, and instead, we propose a method for obtaining even larger gain for smaller slab structures by periodically switching the sign of the applied field E_0 in time with a period equal to $L\mathrm{Re}(k)/\omega$, as depicted in Fig. 4(b). In doing so, the sound field experiences gain in propagating the slab in forward and backward directions since the sign of the damping term $\mathrm{Im}(k)$ as seen in Fig. 4(c) opposes the sign of E_0 and is switched exactly when a wave round-trip is initiated. The effect of the controlled switching can be seen in Fig. 4(d), where the transmission T and reflection R coefficients are shown for cases with (s) and without switching

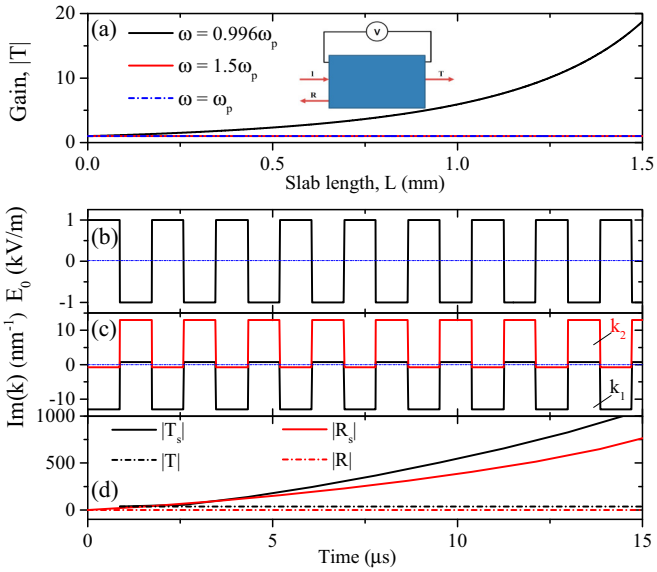

FIG. 4. (Color online) Electrically controlled optomechanical device for acoustic amplification. (a) Transmission coefficient of an incoming sound field plotted as a function of the length of an InSb slab operating near the plasmon frequency. The inset shows a sketch of the optomechanical device. (b) Several cycles of the electric field E_0 where switching is enforced at a period of $L\mathrm{Re}(k)/\omega$. (c) The controlled switching ensures enhanced acoustic gain by periodically changing the sign of $\mathrm{Im}(k)$ during the round-trips of the wave. (d) Transmission (T_s, T) and reflection (R_s, R) coefficients as a function of time in cases with (s) and without switching of E_0. Parameters are $f = 2.69$ THz and $L = 4.8$ mm, and the acoustic impedance of the surrounding media is $Z = 3 \times 10^7$ kg/(m^2 s).

of E_0. Over time, huge transmissions and reflections are built up when switching is imposed. On the other hand, there is no additional amplification of sound in making a slab round-trip for a constant applied field since the gain experienced in propagating forward is lost upon propagating backward.

We have demonstrated how sound amplification in PZ materials can be substantially enhanced when operated at ENZ response. We utilized this finding by designing a switch-controlled optomechanical device producing larger-than-unity scattering coefficients of the radiated sound field, and we foresee that this technique will find many striking applications for sensing and spectroscopy. The fact that acoustic gain can be much higher than realized in the works by White and Hutson [10–12] makes the present idea less sensitive to crystal noise for sound amplification at ENZ conditions, resulting in a high signal-to-noise ratio. To embed this concept in future and current systems, one needs to consider possible saturation of gain as a result of nonlinear sound interaction and increased material absorption. We note also that acoustic dissipation mechanisms play an increasing role at higher frequencies. There are other methods for obtaining acoustic gain, such as parametric amplification in a magnetostrictive solid [17]. Furthermore, we stress that amplification of sound has also been reported in nonclassical systems, giving rise to phonon lasing and amplification in Stark ladder superlattices [18–20]. The present idea, based on the piezoelectric effect that exists in a large class of semiconductors where the unit cell is inversion asymmetric, does not require direct excitation of photons. An incoming acoustic wave will, under the application of a dc electric field, experience amplification. Acoustic amplification can also be generated in the absence of an incoming acoustic wave by applying a dc and an ac electric field component simultaneously. In recent years several intriguing phenomena in acoustic metamaterials have been explored [21–26]. We envision that the present idea of sound amplification could find use in metamaterial-related applications at much lower frequencies, providing active compensation of losses at resonance and the design of audible gain by structuring PZ materials.

J.C. gratefully acknowledges financial support from the Danish Council for Independent Research and a Sapere Aude grant (Grant No. 12-134776).

[1] Z. W. Pan and Z. L. Wang, Science **291**, 1947 (2001).
[2] Z. L. Wang and J. Song, Science **312**, 242 (2006).
[3] Z. L. Wang, Mater. Today **10**, 20 (2007).
[4] Z. L. Wang, Adv. Mater. **19**, 889 (2007).
[5] H. D. Espinosa, R. A. Bernal, and M. Minary-Jolandan, Adv. Mater. **24**, 4656 (2012).
[6] L. C. Lew Yan Voon and M. Willatzen, J. Appl. Phys. **109**, 031101 (2011).
[7] Y. Yang, W. Guo, K. C. Pradel, G. Zhu, Y. Zhou, Y. Zhang, Y. Hu, L. Lin, and Z. L. Wang, Nano Lett. **12**, 2833 (2012).
[8] Y. M. Lin and M. S. Dresselhaus, Phys. Rev. B **68**, 075304 (2003).
[9] J. R. Lim, J. F. Whitacre, J. P. Fleurial, C. K. Huang, M. A. Ryan, and N. V. Myung, Adv. Mater. **17**, 1488 (2005).
[10] A. R. Hutson, J. H. McFee, and D. L. White, Phys. Rev. Lett. **7**, 237 (1961).
[11] D. L. White, J. Appl. Phys. **33**, 2547 (1962).
[12] A. R. Hutson and D. L. White, J. Appl. Phys. **33**, 40 (1962).
[13] V. I. Pustovoit, Sov. Phys. Usp. **12**, 105 (1969).
[14] B. Edwards, A. Alu, M. E. Young, M. Silveirinha, and N. Engheta, Phys. Rev. Lett. **100**, 033903 (2008).
[15] R. Maas, J. Parsons, N. Engheta, and A. Polman, Nat. Photonics **7**, 907 (2013).
[16] N. Engheta, Science **340**, 286 (2013).
[17] A. P. Brysev, L. M. Krutyanskii, and V. L. Preobrazhenskii, Phys. Usp. **41**, 793 (1998).
[18] A. J. Kent, R. N. Kini, N. M. Stanton, M. Henini, B. A. Glavin, V. A. Kochelap, and T. L. Linnik, Phys. Rev. Lett. **96**, 215504 (2006).
[19] R. P. Beardsley, A. V. Akimov, M. Henini, and A. J. Kent, Phys. Rev. Lett. **104**, 085501 (2010).
[20] I. Mahboob, K. Nishiguchi, A. Fujiwara, and H. Yamaguchi, Phys. Rev. Lett. **110**, 127202 (2013).
[21] Z. Liu, X. Zhang, Y. Mao, Y. Y. Zhu, Z. Yang, C. T. Chan, and P. Sheng, Science **289**, 1734 (2000).

[22] J. Christensen, A. I. Fernandez-Dominguez, F. de Leon-Perez, L. Martin-Moreno, and F. J. Garcia-Vidal, Nat. Phys. **3**, 851 (2007).

[23] Y. Xie, B.-I. Popa, L. Zigoneanu, and S. A. Cummer, Phys. Rev. Lett. **110**, 175501 (2013).

[24] M. Kadic, T. Bueckmann, R. Schittny, and M. Wegener, Rep. Prog. Phys. **76**, 126501 (2013).

[25] M. Wegener, Science **342**, 939 (2013).

[26] M. Maldovan, Nature (London) **503**, 209 (2013).